

# Activity-Based Probes for Isoenzyme- and Site-Specific Functional Characterization of Glutathione S-Transferases

Ethan G. Stoddard, Bryan J. Killinger, Reji N. Nair, Natalie C. Sadler, Regan F. Volk, Samuel O. Purvine, Anil K. Shukla, Jordan N. Smith, and Aaron T. Wright\*

Chemical Biology and Exposure Sciences, Biological Sciences Division, Pacific Northwest National Laboratory, 902 Battelle Boulevard, Richland, Washington 99352, United States

## Supporting Information

**ABSTRACT:** Glutathione S-transferases (GSTs) comprise a diverse family of phase II drug metabolizing enzymes whose shared function is the conjugation of reduced glutathione (GSH) to endo- and xenobiotics. Although the conglomerate activity of these enzymes can be measured, the isoform-specific contribution to the metabolism of xenobiotics in complex biological samples has not been possible. We have developed two activity-based probes (ABPs) that characterize active GSTs in mammalian tissues. The GST active site is composed of a GSH binding “G site” and a substrate binding “H site”. Therefore, we developed (1) a GSH-based photoaffinity probe (GSTABP-G) to target the “G site”, and (2) an ABP designed to mimic a substrate molecule and have “H site” activity (GSTABP-H). The GSTABP-G features a photo-reactive moiety for UV-induced covalent binding to GSTs and GSH-binding enzymes. The GSTABP-H is a derivative of a known mechanism-based GST inhibitor that binds within the active site and inhibits GST activity. Validation of probe targets and “G” and “H” site specificity was carried out using a series of competition experiments in the liver. Herein, we present robust tools for the characterization of enzyme- and active site-specific GST activity in mammalian model systems.

Glutathione S-transferases (GSTs) are a diverse group of phase II drug metabolizing enzymes whose shared function is the conjugation of glutathione (GSH) to various electrophilic endo- and xenobiotics.<sup>1</sup> GSTs have been implicated in the conjugation of endogenously produced oxidized metabolites including propenal, 4-hydroxynonenals, organic hydroperoxides, phospholipids, and fatty acid peroxides.<sup>2–5</sup> Reactive species generated by P450 monooxygenation of exogenous polycyclic aromatic hydrocarbons (PAHs) are also conjugated to GSH, highlighting the importance of GSTs in the protection of macromolecules such as DNA or proteins from modification by P450-activated PAH metabolites.<sup>6–8</sup> Additionally, many chemotherapeutic drugs, such as 1,3-bis(2-chloroethyl)-1-nitrosourea and chlorambucil, function as alkylating agents and are inactivated via GSH conjugation.<sup>9–12</sup> Due to their function in the detoxification of endogenous and exogenous electrophiles, an exploration of enzyme-specific response to perturbation is critical for understanding mammalian metabolism of xeno- and endobiotics.

GSTs are categorized by their subcellular location into cytosolic, mitochondrial, and microsomal superfamilies and are further divided into classes based on sequence homology. GSTs contain a GSH binding “G” site and a substrate-binding “H” site. Though the G site is highly conserved, the H site is variable between classes, contributing to interclass diversity in substrate specificity.<sup>1</sup> Expression of GSTs is often nonindicative of the propensity of these enzymes for their detoxifying GSH transferase activity. This discrepancy between expression and activity can be attributed to known post-translational modifications, alternative enzyme-specific nontransferase activities, and activity altering protein–protein interactions.<sup>13–16</sup> Measurement of GST activity using commercial activity assays provides information regarding the total GSH conjugating ability of a system, but fail to reveal enzyme-specific activity. Due to incongruence of GST expression and activity, in combination with a limited toolkit for studying GST activity, robust tools to measure enzyme-specific GST activity are needed.

We developed two probes to enable activity-based protein profiling of GSTs at the GSH-binding G site and the substrate binding H site (Figure 1A), and validated their ability to target and measure the activity of GSTs in mammalian model systems. The first probe (GSTABP-G) was designed to target the GSH-binding G site of GSTs by mimicking GSH (Figure 1B). A photoreactive benzophenone and a terminal alkyne were appended to the thiol of GSH. This allows for irreversible binding of the probe to GST targets when UV irradiated, and the subsequent enrichment of targeted proteins following click chemistry. GST enzymes recognize and bind the peptidic structure of GSH, whose GSH thiol functions as a nucleophile for GST-mediated attachment to xenobiotics. Thus, to target the G site we modified the thiol with the alkyne and benzophenone containing linker. To complement the G site targeting photoaffinity probe, we developed a mechanism-based probe designed to characterize H site activity (Figure 1C). The second probe (GSTABP-H) is derived from Dichlon (2,3-dichloro-1,4-naphthoquinone), a broad spectrum irreversible inhibitor of human and rodent GST isoenzymes.<sup>17,18</sup> We hypothesized that GSTABP-H would bind H sites due to Dichlon’s hydrophobicity and electrophilicity, which are properties of H site binding molecules. In addition, evidence suggests the Dichlon moiety may also have capacity to bind conserved catalytic tyrosines within GST H sites. For example, a GST  $\mu$  isoenzyme has

Received: July 19, 2017

Published: October 25, 2017



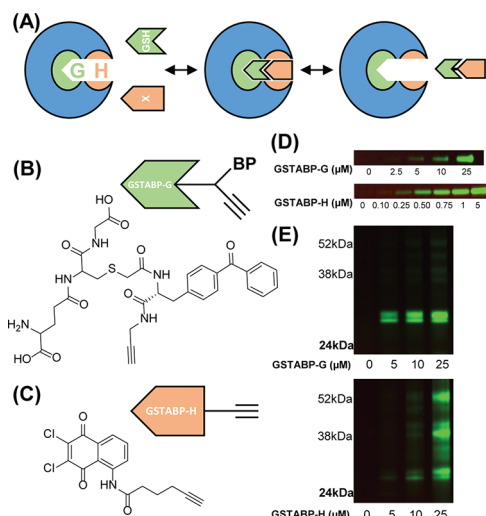


**Figure 1.** Activity- and affinity-based probes designed to target active GSTs. (A) Function of active GSTs; the conjugation of reduced glutathione (GSH) to xenobiotic (X) stabilized by “G” and “H” site binding by each substrate, respectively. (B) Structure of affinity-based GSTABP-G designed to target GST “G” sites. (C) Structure of activity-based GSTABP-H designed to target GST “H” sites. GSTABP-G and GSTABP-H probe dependent labeling of 1  $\mu$ M recombinant human GSTM1 (D) and 1 mg/mL mouse liver cytosol (E). BP: benzophenone.

previously been found to be irreversibly bound by 2-(S-glutathionyl)-3,5,6-trichloro-1,4-benzoquinone. The proposed binding mechanism involves an interaction between the catalytic tyrosines and the chlorinated quinone moiety shared by 2-(S-glutathionyl)-3,5,6-trichloro-1,4-benzoquinone and Dichlon.<sup>19</sup> Thus, we posited an alkyne-appended Dichlon derivative would make an effective H site targeting activity-based probe (ABP).

To validate irreversible labeling of active GSTs by the ABPs, we first evaluated concentration dependent labeling of a recombinant GST. GSTABP-G and GSTABP-H were applied with increasing concentrations to the recombinant human GSTM1, a GST isoenzyme that is highly expressed in mammalian liver. After 30 min of incubation, a fluorescent rhodamine reporter was added by click chemistry, and SDS-PAGE revealed both probes exhibit concentration-dependent labeling of GSTM1 (Figure 1D). Both probes were then applied with increasing concentrations to the cytosolic fraction of mouse liver lysate to further test probe targeting. Both probes strongly label two distinct bands at 24 kDa (Figure 1E). The lower band is likely GSTP1, a 23.6 kDa protein highly abundant in the liver. The upper band shows probable GST targets from the  $\mu$  and  $\alpha$  classes, the molecular weights of which are  $\sim$ 26 kDa. In addition to these proteins, the GSTABP-H shows concentration-dependent labeling of various higher molecular weight proteins. Though GSTABP-G demonstrates high selectivity, GSTABP-H seems more susceptible to off-target labeling, likely due to its strong electrophilic nature (Figure 1E). To determine the specific GST isoforms targeted by each probe, we performed LC-MS-based proteomics analyses of mouse liver labeling, and labeling in the presence of specific inhibitors (Figure 2). Proteomics revealed that GSTABP-G shows high specificity for GSTs (Figure 2A). Twenty-seven probe-targeted proteins were determined to be statistically significant targets of GSTABP-G at a fold-change of 3 over no UV exposure controls. Of these 27 proteins, eight are GSTs and include members of  $\mu$ ,  $\alpha$ ,  $\pi$ ,  $\theta$ ,  $\kappa$ , and  $\zeta$  classes. The remaining proteins include five

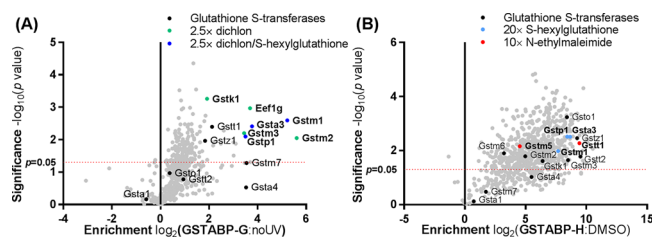


**Figure 2.** LC-MS/MS chemoproteomics results of probe enriched and probe competed mouse liver cytosol ( $n = 3$ ). All samples were incubated with 10  $\mu$ M probe or an equal concentration of vehicle control. Enrichment was calculated as AMT tag abundances from probe-enriched samples divided by a no UV (for GSTABP-G) or DMSO only (for GSTABP-H) control. Significance was determined using a paired  $t$  test with a two-tailed distribution. (A) Volcano plot of GSTABP-G enrichment. In black: all GSTs that did not demonstrate competitive inhibition of probe labeling. In green: GSTs whose probe labeling was competitively inhibited by 2.5 $\times$  excess 2,3-dichloro-1,4-naphthoquinone (Dichlon) over probe. In blue: GSTs whose probe labeling was competitively inhibited by 2.5 $\times$  excess Dichlon and 2.5 $\times$  excess S-hexylglutathione. (B) Volcano plot of GSTABP-H enrichment. In black: all GSTs whose probe labeling was not competitively inhibited. In blue: GSTs whose probe labeling was competitively inhibited by 20 $\times$  S-hexylglutathione. In red: GSTs whose probe labeling was competitively inhibited by 10 $\times$  N-ethylmaleimide.

proteins with known GSH binding, one with known antioxidant and drug binding activity, and five proteins highly abundant in liver with no known GSH binding activity (SI Table S1). GSTABP-H also facilitated enrichment of 12 members of the GST  $\mu$ ,  $\alpha$ ,  $\pi$ ,  $\theta$ ,  $\omega$ ,  $\kappa$ , and  $\zeta$  classes (Figure 2B; SI Table S2). However, as with the gel studies, proteomics results for GSTABP-H indicate considerably more off-target labeling than GSTABP-G. An evaluation of the off-targets reveals that many of these proteins have known reactive thiols, akin to many GSTs. These results validate the effectiveness of both probes for isoenzyme-specific targeting of many members of cytosolic GST classes. To demonstrate the selectivity of the probes, and the value of an ABP approach over global abundance profiling, we compared ABP labeling results to global proteomics analysis of liver lysate. Only six GSTs were identified by global analysis, but ABP-labeling resulted in the detection of 12 GSTs, including all of the GSTs detected in unenriched lysate (SI Table S3). Thus, in contrast to global analyses, the ABPs enable characterization of active and low abundance GSTs.

To distinguish between activity-specific binding and general reactivity of the probes, and to characterize their selectivity for G or H site specificity, we competed GSTABP-H and GSTABP-G labeling of mouse liver lysate against relevant inhibitors. To evaluate G site labeling by GSTABP-G, GSH was added in excess. Gel and LC-MS analysis showed no significant inhibition (data not shown). We hypothesize this lack of inhibition is attributable to the formation of glutathione disulfides (GS-SG) in our *in vitro* proteome sample. To circumvent the requisite addition of potentially activity-modifying reducing agents to prevent GS-SG formation, we competed probe labeling with S-hexylglutathione, a GSH conjugate incapable of forming disulfide bonds. S-Hexylglutathione inhibits GSTABP-G labeling of GSTs in a concentration dependent manner, with an effective concentration of 1.77  $\mu$ M (to 10  $\mu$ M probe), suggestive of GSTABP-G specificity for the G site (Figure 3).

To investigate GSTABP-H targeting of GST H sites, we compared competition of GSTABP-H with the G site inhibitor S-hexylglutathione to competition with ethacrynic acid, a known

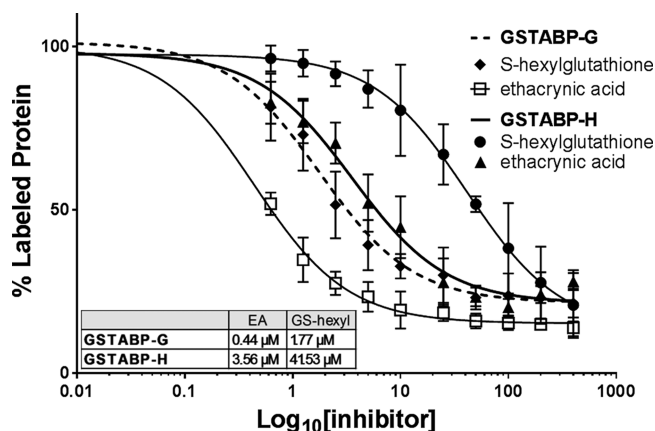


**Figure 3.** Competitive inhibition of GSTABP-G and GSTABP-H labeling of mouse liver cytosol to delineate G and H site binding ( $n = 3$ ). 10  $\mu$ M probe was used in all samples. Increasing concentrations of S-hexylglutathione (GS-hexyl) or ethacrynic acid (EA) was incubated with mouse liver cytosol for 30 min before probe labeling for 30 min. Afterward, rhodamine was attached to the probe–protein complexes via click chemistry. Proteins were resolved via SDS-PAGE followed by fluorescence gel imaging and quantification (arbitrary units) of probe labeled GST bands. All replicates were normalized to a % labeled protein value (probed samples with no inhibitor = 100%). Normalized values were plotted and  $EC_{50}$  values were determined with a best fit curve.

H site inhibitor.<sup>20–23</sup> S-Hexylglutathione shows significant inhibition of GSTABP-H labeling with an  $EC_{50}$  of 41.5  $\mu$ M (Figure 3). It is plausible this competition is due to a known interaction between S-hexylglutathione's conjugated hexyl moiety and the GST H site.<sup>24</sup> Although our G site inhibitor decreases GSTABP-H binding, we expected the H site inhibitor, ethacrynic acid, to be much more effective. We found ethacrynic acid to be nearly 12 $\times$  more potent in inhibiting GSTABP-H enzyme labeling compared to S-hexylglutathione, indicating that GSTABP-H selectively targets GST H sites (Figure 3). Ethacrynic acid also competed GSTABP-G labeling with an  $EC_{50}$  of 0.44  $\mu$ M. Thus, ethacrynic acid may block both GSTABP-G and GSTABP-H access to the G site (Figure 3). It is also possible that the presence of ethacrynic acid in the H site interferes with the alkyne and benzophenone moieties of GSTABP-G that likely reside in the H site.

To confirm active site-specific probe labeling of GSTs and GSH-binding proteins, we performed proteomic analysis of S-hexylglutathione competition in liver cytosol. GSTABP-H and GSTABP-G labeling of GSTA3, M1, and P1 was significantly inhibited by S-hexylglutathione (fold change > 3.0,  $p \leq 0.05$ ), and were the top three of all inhibited targets when sorted by fold-change repression, indicating that both probes are labeling the active site of GSTs (Figure 2; SI Table S4; SI Table S5).

The subsite complementarity of the probes provide a unique approach to examine each probe's enzyme specificity. For example, we postulated Dichlon could effectively inhibit GSTABP-G labeling by physically competing the alkyne and benzophenone moieties that likely extend into the H site, as with S-hexylglutathione. Congruent with this hypothesis, we showed that competition with Dichlon in mouse liver cytosol selectively inhibits labeling of a 24 kDa protein, the approximate weight of several GSTs (Figure S1). Additionally, LC-MS was performed on Dichlon competed GSTABP-G labeled mouse liver cytosol and revealed labeling of GSTP1, M4, A3, M1, K1, and M2 was significantly competed by Dichlon ( $FC > 2$ ,  $p \leq 0.05$ ) (Figure 2A). This indicates that the GSTABP-H parent Dichlon

molecule selectively inhibits a variety of GST classes near the same binding region as the GSTABP-G, further confirming that the GSTABP-H is binding to the active site of GSTs. To investigate the impact of the alkyne on the reactivity of GSTABP-H's Dichlon moiety, we competed GSTABP-H labeling of liver cytosol with Dichlon (Figure S1). Inhibition resulted in decreases in all measurable fluorescent bands, indicating that the alkyne does not significantly affect reactivity.

Finally, to differentiate between the general reactivity of the GSTABP-H versus its activity-specific labeling, we performed competitive probe labeling using N-ethylmaleimide (NEM), a cysteine alkylating agent. Proteomic analysis of 100  $\mu$ M NEM competed GSTABP-H labeling failed to compete for binding of most GST isoenzymes, indicating cysteine binding may not be the primary amino acid targeted by GSTABP-H (Figure 2B; SI Table S5). In combination with previous studies suggesting tyrosine binding by chlorinated quinones,<sup>19</sup> these results are suggestive that tyrosine may be the primary residue irreversibly bound by GSTABP-H.

Following our investigation into the labeling mechanisms of the ABPs, we evaluated changes in site-specific GST activity of organs relevant to xenobiotic metabolism including liver, lung, kidney, intestine, spleen, and heart lysates.<sup>25</sup> We compared GST activity determined via probe labeling and fluorescence gel imaging with a colorimetric GST activity assay that measures the total conglomerate of GST activity. Fluorescence intensity of ABP labeling was determined by quantification of the fluorescence signal. As anticipated, liver GST activity was highest by ABP labeling, followed by lung and kidney. These measurements closely correspond with total GST activity determined by the assay (Figure S2). We then conducted proteomics studies on lung lysate. Eleven GST isoenzymes were enriched by GSTABP-H, and 3 GST enzymes were enriched by GSTABP-G (Figure 4A; SI Table S6). Both probes showed high

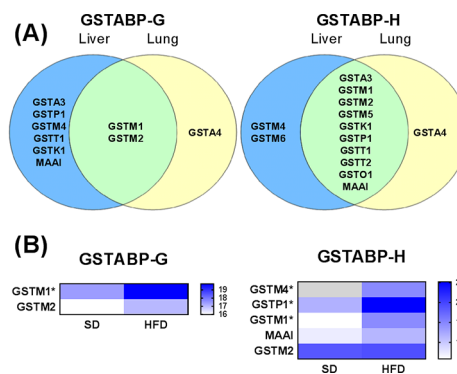


**Figure 4.** (A) Liver and lung GSTABP-G and GSTABP-H targets (from probe enrichment and LC-MS/MS analysis) depicted as a Venn diagram. (B) Heatmap depicting relative abundances of GSTABP-G and GSTABP-H GST targets in hepatic cytosol from untreated versus corn oil treated mice. Proteins with asterisk denotes significant alteration in protein abundance from SD to HFD mice based on student's t-test and fold change abundances (fold change > 2.0,  $p \leq 0.05$ ).

enrichment of lung GSTA4, a protein not significantly enriched by either probe in liver lysate, as anticipated from prior studies.<sup>25</sup> Though GSTABP-H and GSTABP-G show enrichment of GSTM4 in the liver, no activity was detected in lung lysate. GSTABP-H also enriches GSTM6 in liver lysate, but not lung. This data is consistent with mRNA expression analyses<sup>25</sup> and demonstrates the effectiveness of these complementary probes



to examine the tissue-specific contribution of GSTs in xenobiotic metabolism.

Finally, to validate that the probes detect physiologically relevant alterations to GST activity, we compared ABP-determined GST activity in intestines of mice fed standard (10% fat) or high fat, obesogenic, chow (60% fat) over a 20 week period. Statistically significant alterations in several GST isoenzymes were seen in response to diet induced obesity, including members of  $\mu$  and  $\pi$  GST classes (Figure 4B; SI Table S7). The activity increases in intestinal GSTs in obese mice is likely a response to oxidative stress resulting from obesity.<sup>26</sup>

We anticipate that successful targeting of GSTs in mammalian model systems by ABPs will enable a much improved understanding of the role of GSTs in human drug metabolism and xenobiotic exposure. The GSH-conjugating activity of GSTs is affected by various factors, including PTMs, making transcriptomics and global proteomics poor indicators of activity. The ability to analyze the enzyme-specific activity of GSTs is required to advance investigations into the pathways involved in GSH conjugation. Of the 19 cytosolic mammalian GSTs encoded in the genome, the probes successfully label 13, demonstrating that the ABPs can broadly profile individual GST activities. The ABPs also facilitate enrichment of members of all GST classes. Probe labeling and MS analysis of other tissues in which the remaining GSTs show higher activity may reveal comprehensive cytosolic GST targeting. We assert that this chemoproteomics approach, using these complementary activity- and affinity-based probes, provides a required advance for understanding of human drug metabolism and response to exposure.

## ■ ASSOCIATED CONTENT

### ■ Supporting Information

The Supporting Information is available free of charge on the ACS Publications website at DOI: 10.1021/jacs.7b07378.

Experimental details (PDF)  
GSTABP-G Targets in Murine Liver (XLSX)  
GSTABP-H Targets in Murine Liver (XLSX)  
GSTs: global vs. ABP-enriched (XLSX)  
Competitively Inhibited GSTABP-G (XLSX)  
Competitively Inhibited GSTABP-H (XLSX)  
GSTABP Targets in Murine Lung (XLSX)  
GSTABP Targets in DIO Murine Intestine (XLSX)

## ■ AUTHOR INFORMATION

### Corresponding Author

\*aaron.wright@pnnl.gov

### ORCID

Aaron T. Wright: 0000-0002-3172-5253

### Notes

The authors declare no competing financial interest.  
The mass spectrometry proteomics data have been deposited to the ProteomeXchange Consortium via the PRIDE partner repository with the data set identifier PXD006920 and 10.6019/PXD006920.

## ■ ACKNOWLEDGMENTS

This research was supported by the National Institutes of Health National Institute of Environmental Health Sciences (P42 ES016465), and employed proteomics capabilities supported by the NIH NIGMS Research Resource for Integrative Biology

(P41 GM103493). A portion of the research was performed using EMSL, a DOE Office of Science User Facility sponsored by the Office of Biological and Environmental Research. PNNL is a multiprogram laboratory operated by Battelle for U.S. DOE Contract DE-AC06-76RL01830.

## ■ REFERENCES

- (1) Armstrong, R. N. *Compr. Tox.* **2010**, 295.
- (2) Danielson, U. H.; Esterbauer, H.; Mannervik, B. *Biochem. J.* **1987**, 247, 707.
- (3) Berhane, K.; Widersten, M.; Engström, A.; Kozarich, J. W.; Mannervik, B. *Proc. Natl. Acad. Sci. U. S. A.* **1994**, 91, 1480.
- (4) Singhal, S. S.; Singh, S. P.; Singhal, P.; Horne, D.; Singhal, J.; Awasthi, S. *Toxicol. Appl. Pharmacol.* **2015**, 289, 361.
- (5) Singhal, S. S.; Zimniak, P.; Awasthi, S.; Piper, J. T.; He, N. G.; Teng, J. I.; Petersen, D. R.; Awasthi, Y. C. *Arch. Biochem. Biophys.* **1994**, 311, 242.
- (6) Hu, X.; Srivastava, S. K.; Xia, H.; Awasthi, Y. C.; Singh, S. V. *J. Biol. Chem.* **1996**, 271, 32684.
- (7) Kabler, S. L.; Seidel, A.; Jacob, J.; Doehmer, J.; Morrow, C. S.; Townsend, A. J. *Chem.-Biol. Interact.* **2009**, 179, 240.
- (8) Morgenstern, R.; DePierre, J. W.; Lind, C.; Guthenberg, C.; Mannervik, B.; Ernster, L. *Biochem. Biophys. Res. Commun.* **1981**, 99, 682.
- (9) Morrow, C. S.; Smitherman, P. K.; Diah, S. K.; Schneider, E.; Townsend, A. J. *J. Biol. Chem.* **1998**, 273, 20114.
- (10) Meyer, D. J.; Gilmore, K. S.; Harris, J. M.; Hartley, J. A.; Ketterer, B. *Br. J. Cancer* **1992**, 66, 433.
- (11) Larsson, A.-K.; Shokeer, A.; Mannervik, B. *Arch. Biochem. Biophys.* **2010**, 497, 28.
- (12) Ali-Osman, F.; Caughlan, J.; Gray, G. S. *Cancer Res.* **1989**, 49, 5954.
- (13) Townsend, D. M.; Manevich, Y.; He, L.; Hutchens, S.; Pazoles, C. J.; Tew, K. D. *J. Biol. Chem.* **2009**, 284, 436.
- (14) Board, P. G.; Coggan, M.; Chelvanayagam, G.; Easteal, S.; Jermini, L. S.; Schulte, G. K.; Danley, D. E.; Hoth, L. R.; Griffor, M. C.; Kamath, A. V.; Rosner, M. H.; Chrzynek, B. A.; Perregaux, D. E.; Gabel, C. A.; Geoghegan, K. F.; Pandit, J. *J. Biol. Chem.* **2000**, 275, 24798.
- (15) Theodoratos, A.; Blackburn, A. C.; Coggan, M.; Cappello, J.; Larter, C. Z.; Matthaei, K. I.; Board, P. G. *Int. J. Obes.* **2012**, 36, 1366.
- (16) Singh, S. *Cancer Chemother. Pharmacol.* **2015**, 75, 1.
- (17) van Ommen, B.; Ploemen, J. H.; Bogaards, J. J.; Monks, T. J.; Gau, S. S.; van Bladeren, P. J. *Biochem. J.* **1991**, 276, 661.
- (18) Vos, R. M. E.; Van Ommen, B.; Hoekstein, M. S. J.; De Goede, J. H. M.; Van Bladeren, P. J. *Chem.-Biol. Interact.* **1989**, 71, 381.
- (19) Ploemen, J. H.; Johnson, W. W.; Jespersen, S.; Vanderwall, D.; van Ommen, B.; van der Greef, J.; van Bladeren, P. J.; Armstrong, R. N. *J. Biol. Chem.* **1994**, 269, 26890.
- (20) Ploemen, J. H.; van Ommen, B.; Bogaards, J. J.; van Bladeren, P. J. *Xenobiotica* **1993**, 23, 913.
- (21) Ploemen, J. H.; van Ommen, B.; van Bladeren, P. J. *Biochem. Pharmacol.* **1990**, 40, 1631.
- (22) Cameron, A. D.; Sinning, I.; L'Hermite, G.; Olin, B.; Board, P. G.; Mannervik, B.; Jones, T. A. *Structure* **1995**, 3, 717.
- (23) Oakley, A. J.; Rossjohn, J.; Lo Bello, M.; Caccuri, A. M.; Federici, G.; Parker, M. W. *Biochemistry* **1997**, 36, 576.
- (24) Reinemer, P.; Dirr, H. W.; Ladenstein, R.; Huber, R.; Lo Bello, M.; Federici, G.; Parker, M. W. *J. Mol. Biol.* **1992**, 227, 214.
- (25) Knight, T. R.; Choudhuri, S.; Klaassen, C. D. *Toxicol. Sci.* **2007**, 100, 513.
- (26) Marseglia, L.; Manti, S.; D'Angelo, G.; Nicotera, A.; Parisi, E.; Di Rosa, G.; Gitto, E.; Arrigo, T. *Int. J. Mol. Sci.* **2015**, 16, 378.